Nonsurgical treatment of skin cancer with local delivery of bioadhesive nanoparticles

Jamie K. Hu[a], Hee-Won Suh[b], Munibah Qureshi[a], Julia M. Lewis[a], Sharon Yaqoob[a], Zoe M. Moscato[b], Sofia Griff[b], Alison K. Lee[a], Emily S. Yin[a], W. Mark Saltzman[b], and Michael Girardi[a,1]

[a]Department of Dermatology, School of Medicine, Yale University, New Haven, CT 06520; and [b]Department of Biomedical Engineering, School of Engineering and Applied Science, Yale University, New Haven, CT 06511

Edited by Joseph M. DeSimone, Stanford University, Stanford, CA, and approved January 5, 2021 (received for review October 6, 2020)

Keratinocyte-derived carcinomas, including squamous cell carcinoma (SCC), comprise the most common malignancies. Surgical excision is the therapeutic standard but is not always clinically feasible, and currently available alternatives are limited to superficial tumors. To address the need for a nonsurgical treatment for nodular skin cancers like SCC, we developed a bioadhesive nanoparticle (BNP) drug delivery system composed of biodegradable polymer, poly(lactic acid)-hyperbranched polyglycerol (PLA-HPG), encapsulating camptothecin (CPT). Nanoparticles (NPs) of PLA-HPG are nonadhesive NPs (NNPs), which are stealthy in their native state, but we have previously shown that conversion of the vicinal diols of HPG to aldehydes conferred NPs the ability to form strong covalent bonds with amine-rich surfaces. Herein, we show that these BNPs have significantly enhanced binding to SCC tumor cell surfaces and matrix proteins, thereby significantly enhancing the therapeutic efficacy of intratumoral drug delivery. Tumor injection of BNP-CPT resulted in tumor retention of CPT at ∼50% at 10 d postinjection, while CPT was undetectable in NNP-CPT or free (intralipid) CPT-injected tumors at that time. BNP-CPT also significantly reduced tumor burden, with a portion (∼20%) of BNP-CPT–treated established tumors showing histologic cure. Larger, more fully established PDV SCC tumors treated with a combination of BNP-CPT and immunostimulating CpG oligodeoxynucleotides exhibited enhanced survival relative to controls, revealing the potential for BNP delivery to be used along with local tumor immunotherapy. Taken together, these results indicate that percutaneous delivery of a chemotherapeutic agent via BNPs, with or without adjuvant immunostimulation, represents a viable, nonsurgical alternative for treating cutaneous malignancy.

squamous cell carcinoma | drug delivery | nanoparticle | chemotherapy | immunotherapy

In the United States, the frequency of skin malignancies exceeds the frequency of all other cancers combined (1). Keratinocyte-derived carcinomas (KDCs), such as cutaneous squamous cell carcinoma (SCC), comprise the most common class of these malignancies, with SCCs responsible for ∼5 million cases and 10,000 deaths annually in the United States (2, 3). The incidence of cutaneous SCC has been steadily rising, with some estimates reporting greater than a 250% increase from 1976 to 1984 and 2000 to 2010 (4, 5). These numbers are projected to rise in proportion to the expanding elderly population, as well as the number of immunocompromised patients living with advanced disease (6–8), posing a significant public health challenge.

Surgical excision is the most common first-line treatment for cutaneous SCC (9). However, SCC recurrence is common, with one study reporting rates as high as 50% of patients (10). Furthermore, surgical excision is undesirable in certain clinical settings, including at-risk patients with underlying bleeding diatheses and large-diameter tumors requiring complicated wound closures that increase the potential for postsurgical complications. The management and treatment of KDCs accounts for over $8.1 billion in US healthcare expenditures annually, a significant burden on both individuals and healthcare systems, necessitating efficient and effective alternatives (11, 12).

Although both topical chemotherapeutic and immunomodulatory agents have demonstrated potential in the local treatment of superficial SCCs (13–16), cream and gel formulations fail to achieve adequate penetration into deeper (e.g., nodular) SCCs. Moreover, topical chemotherapy (e.g., 5-fluorouracil) and immunotherapy (e.g., imiquimod) can diffuse from the site of application into the dense vasculature within tumors, with potential for diminished local efficacy and systemic toxicity (17). Thus, additional strategies for local drug delivery are warranted.

Nanoparticles (NPs) formed from the block copolymer poly(lactic acid)-hyperbranched polyglycerol (PLA-HPG) have been shown to increase the duration, bioavailability, and efficacy of locally administered chemotherapy drugs, which minimizes the systemic toxicity associated with conventional chemotherapies (18, 19). PLA-HPG NPs are produced as nonadhesive nanoparticles (NNPs) that can then be transformed into bioadhesive nanoparticles (BNPs) by a brief incubation with sodium periodate (18) (Fig. 1*A*). This treatment alters the chemistry of the surface HPG molecules, converting the vicinal diols to aldehydes, which are capable of forming strong, covalent bonds with amines on the tumor cell surface and tumor interstitial matrix proteins. We have previously shown that this bioadhesive effect leads to durable association of BNPs with cells (18), stratum

Significance

One in five individuals in the United States will develop skin cancer over the course of a lifetime, and nonsurgical options are limited. To address this, we developed a bioadhesive nanoparticle (BNP) treatment for long-lasting local drug delivery. Incorporation of the topoisomerase inhibitor camptothecin (CPT) into BNPs enhanced tumor cell uptake, bioadhesion within the tumor microenvironment, and prolonged intratumoral drug retention. Therefore, we investigated BNPs encapsulating CPT as a local, nonsurgical treatment for nodular squamous cell carcinoma (SCC) skin cancers in a mouse model. BNP-CPT treatment facilitated tumor destruction and resolution, and was compatible with local immunotherapy. These findings suggest that BNP delivery of antitumor agents may provide opportunities for nonsurgical treatment of nodular skin cancers like SCC.

Author contributions: J.K.H., H.-W.S., J.M.L., W.M.S., and M.G. designed research; J.K.H., H.-W.S., M.Q., J.M.L., S.Y., Z.M.M., S.G., A.K.L., and E.S.Y. performed research; J.K.H., H.-W.S., M.Q., J.M.L., S.Y., Z.M.M., S.G., A.K.L., and E.S.Y. analyzed data; and J.K.H., J.M.L., W.M.S., and M.G. wrote the paper.

Competing interest statement: W.M.S. and M.G. have an ownership interest in and are paid consultants with Stradefy Biosciences, Inc.

This article is a PNAS Direct Submission.

[1]To whom correspondence may be addressed. Email: michael.girardi@yale.edu.

This article contains supporting information online at https://www.pnas.org/lookup/suppl/doi:10.1073/pnas.2020575118/-/DCSupplemental.

Published February 1, 2021.

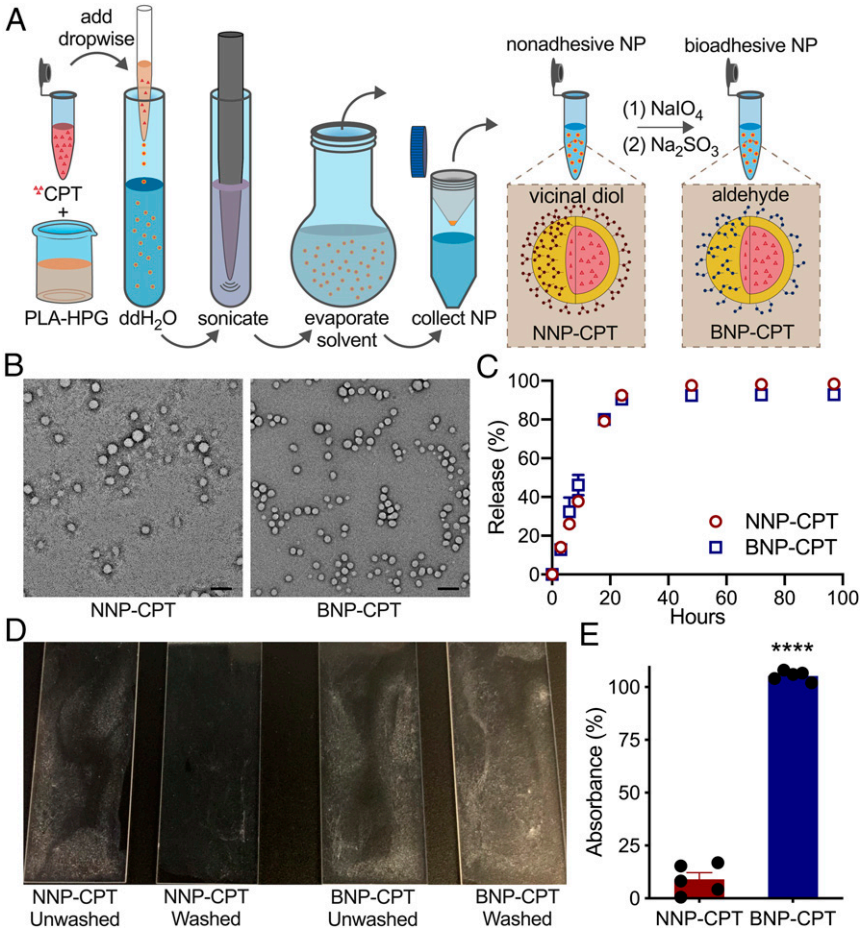

Fig. 1. Synthesis and bioadhesion of CPT-loaded PLA-HPG NNPs and BNPs. (*A*) NP synthesis schematic. (*B*) Transmission electron microscopy images of NNP-CPT and BNP-CPT particles. Following NNP oxidation with sodium periodate, BNPs retain their spherical morphology, indicating that conversion does not compromise the structure of the BNPs. (Scale bar: 100 nm.) (*C*) CPT-loaded NNPs and BNPs show similar temporal drug release kinetics in 1× PBS at 37 °C. Both NNP-CPT and BNP-CPT show the gradual release of drug over 24 h. (*D*) Quantification of bioadhesion of NNPs and BNPs in proteinaceous environments following rigorous washing. When quantifying bioadhesion, (*E*) BNP-CPT demonstrated superior adherence compared to NNP-CPT. Data normalized to unwashed controls. ****$P < 0.0001$, Student's *t* test; $n = 5$.

corneum (20), mesenteric membranes (18), vaginal epithelium (21), and intracranial tumor cells (19). We have also shown that BNPs, applied as a topical sunscreen, can prevent the double-stranded DNA breaks associated with cutaneous carcinogenesis, while at the same time minimizing the systemic accumulation of ultraviolet filters common to commercially available sunscreens (20, 22). For these reasons, we studied the potential role for BNP in a well-characterized, transplantable PDV SCC tumor murine model (23).

Camptothecin (CPT) is a DNA topoisomerase I inhibitor and potent chemotherapy whose functionality is limited by its hydrophobicity and poor solubility, rapid physiological inactivation, and high risk for systemic toxicity (24). Herein, we demonstrate that encapsulation of CPT within BNPs (BNP-CPT) enhances the delivery of CPT, resulting in greater tumor cell uptake, tumor drug retention, and tumor elimination relative to free (intralipid) drug or NNP-encapsulated CPT (NNP-CPT) controls. Given the importance of combination chemotherapeutic and immunomodulatory therapy for cancer, we also examined the efficacy of BNP-encapsulated CPT in combination with adjuvant immune modulation in the form of cytidine-phosphate-guanosine oligodeoxynucleotides (CpGs) to reveal the potential advantages of this combination strategy.

Results

BNP-CPT Synthesis and Characterization. After formation of NNP-CPT, and their subsequent modification to BNP-CPT (Fig. 1*A*), both NNP-CPT and BNP-CPT demonstrated an average size distribution between 200 and 300 nm by dynamic light scattering, demonstrating consistent conversion without significant changes to the hydrodynamic size (*SI Appendix*, Table S1). We confirmed the largely uniform and spherical structure of these PLA-HPG NPs using transmission electron microscopy, and that the oxidative conversion of NNP-CPT to BNP-CPT did not negatively alter the morphology (Fig. 1*B*).

We next analyzed the in vitro kinetics of drug release at physiological temperature (37 °C), observing a sustained and maximal (~90%) release from both NNPs and BNPs over 24 h (Fig. 1*C*). To simulate the protein-rich tumor microenvironment, we prepared poly-L-lysine–coated slides, incubated them with aqueous suspensions of either NNP-CPT or BNP-CPT, and quantified the relative adherence based on the amount of CPT recovered from the slides after washing (Fig. 1*D*). Virtually all of the CPT was recovered when encapsulated in BNPs, compared to a ~10% recovery rate when encapsulated within NNPs (Fig. 1*E*).

BNP Encapsulation Increases Tumor Cell Binding and Uptake. To assess whether the increased bioadhesion from BNP conversion results in greater association with tumor cells, we incubated murine SCC cells (PDVC57) with NNPs or BNPs incorporating a fluorescent dye (DiD). By confocal microscopy, we observed

extensive adhesion of BNPs around and within the SCC cells relative to dye-containing NNP (Fig. 2*A* and *SI Appendix*, Fig. S1). We further assessed the binding affinity of BNP-CPT by incubating PDVC57 cells with Cy5-conjugated NPs or DiD-loaded NPs prior to measuring cellular association as a function of time via flow cytometry. Because BNP may bind serum proteins found in cell culture media, and this could affect NP association with tumor cells, we compared NNP-Cy5 and BNP-Cy5 tumor cell association following short-term culture in serum-containing vs. serum-free media (*SI Appendix*, Fig. S2). In serum-free media (Fig. 2*B* and *SI Appendix*, Fig. S2), BNPs associated with tumor cells to a greater extent than NNPs, and this was most pronounced at later time points (12 to 24 h). In serum-containing media (Fig. 2*C* and *SI Appendix*, Fig. S2), at early time points (up to 5 h) no BNP advantage was seen; however, with extended culture (24 to 72 h), BNPs show significantly greater tumor cell association than NNPs. This was true regardless of whether the dye was covalently conjugated to the polymer (Cy5) or encapsulated within (DiD) the particles (Fig. 2 *B* and *C*). BNP binding to serum proteins may initially slow tumor cell uptake in vitro. Alternatively, cells may respond to the absence of serum by activating additional uptake mechanisms. Because extracellular proteins may also play a role in vivo, we elected to use serum-containing media for the following experiments designed to investigate NP uptake mechanisms.

Cellular association or uptake of NPs occurs via an active process given that tumor cell incubation with NNP or BNP at 4 °C results in significantly reduced cellular association as compared to 37 °C (Fig. 3*A*). We selectively blocked either clathrin-mediated endocytosis or macropinocytosis by applying drugs during incubation with BNPs or NNPs. We found a significant decrease in NNP uptake after blocking either clathrin-mediated endocytosis or macropinocytosis (Fig. 3*B*). In contrast, only interruption of clathrin-mediated endocytosis resulted in a significant decrease in uptake of BNPs in this assay. Overall, these data suggest that BNPs may preferentially utilize clathrin-mediated entry, while NNPs display more promiscuity in cellular entry.

Extracellular Proteins Facilitate Tumor Cell Killing by BNP-CPT. To assess the advantages of bioadhesion, we conducted further in vitro cytotoxicity studies in a simulated tumor matrix (*SI Appendix*, Fig. S3*A*). After precoating 96-well plates with poly-L-lysine, we incubated the plates with either free CPT, NNP-CPT, BNP-CPT, or unloaded NPs (NNP-blank, BNP-blank) for an hour before aspirating the contents and seeding PDVC57 tumor cells into the pretreated wells. After an additional 48-h incubation, we found that BNP-CPT exhibited significantly greater cellular toxicity, when compared to free CPT or NNP-CPT (Fig. 3*C*). Neither unloaded NNPs or unloaded BNPs demonstrated any tumor cell cytotoxicity, indicating that all BNP antitumor effects were attributable to the CPT provided by the

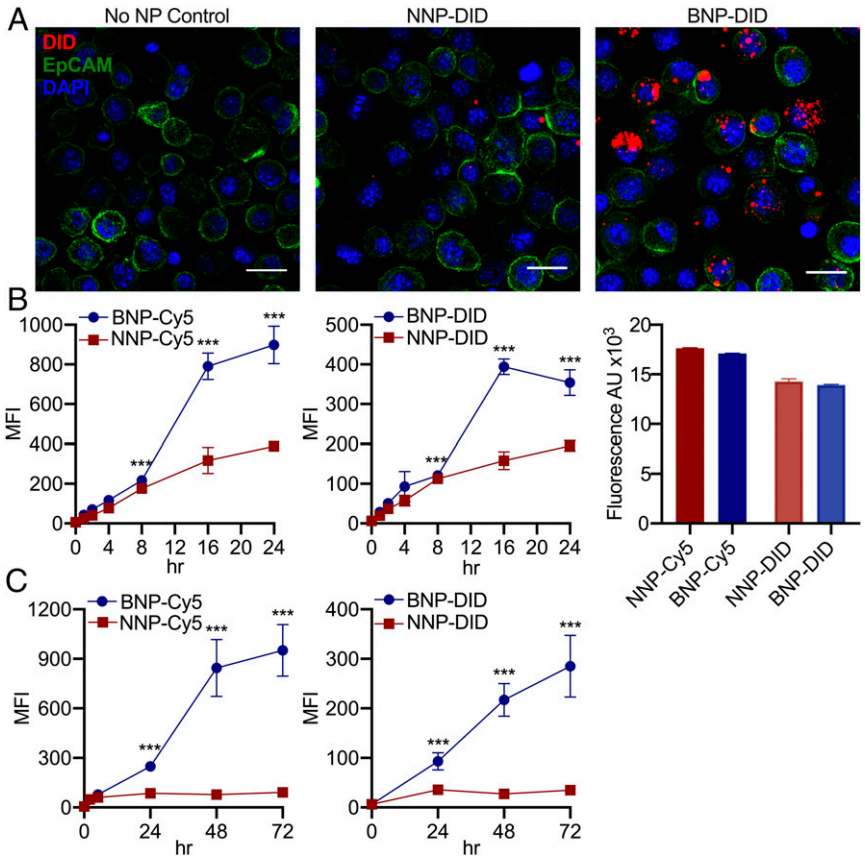

Fig. 2. BNPs readily associate with tumor cells. (*A*) Confocal microscopy of PDV SCC cells following 24-h incubation with DiD dye-loaded NNPs and BNPs demonstrate superior affinity of BNPs to tumor cells. (Scale bar: 20 μm.) (*B*) Assessment of cellular association over time via flow cytometric analysis of PDV cultured under serum-free conditions with Cy5-conjugated NPs (*Left*) and DiD-loaded NPs (*Center*) demonstrates significantly improved association of BNP in both cases, with their advantage especially notable at later time points (16 to 24 h). Baseline fluorescence (*Right*) of both dye-conjugated (Cy5) and -loaded (DiD) NNP and BNP before incubation is similar. A comparison of NP association with tumor cells following short (up to 5 h) incubation in serum-containing vs. serum-free conditions is shown in *SI Appendix*, Fig. S2. (*C*) Cellular association of Cy5-NPs (*Left*) and DiD-NPs (*Right*) with extended incubation in serum-containing media. Even with prolonged exposure, BNPs associate with tumor cells more strongly than NNPs. MFI, mean fluorescence intensity; $n = 3$ replicates. $^{***}P < 0.001$, Student's t test.

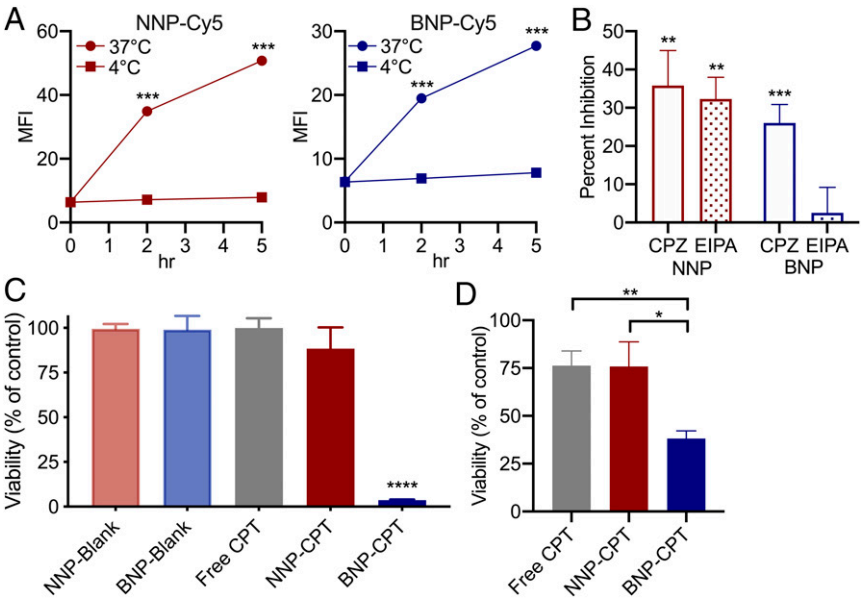

Fig. 3. BNPs facilitate both active internalization by tumor cells and binding to extracellular proteins to promote cytotoxicity. (*A*) Effects of temperature on NNP-Cy5 (*Left*) and BNP-Cy5 (*Right*) association with tumor cells. PDV cells cultured with either NNP-Cy5 or BNP-Cy5 at 4 °C in serum-containing media show only minimal cellular association, whereas 37 °C cultures show significant NP association over time, suggesting active cellular processes are required. MFI, mean fluorescence intensity; $n = 3$. (*B*) Interrogation of clathrin- or macropinocytosis-mediated mechanisms of cellular uptake. Cells were cultured in serum-containing media with NNP-Cy5 or BNP-Cy5 for 16 h and during the final 6 h of culture, vehicle (DMSO, 0.1%), CPZ (20 μM), or EIPA (50 μM) added. Results are expressed as the percent inhibition of NP uptake relative to vehicle control; $n = 3$. (*C*) Poly-L-lysine–coated plates were incubated with blank (unloaded) NP, free CPT, NNP-CPT, or BNP-CPT for 1 h. These solutions were then aspirated and PDVC57 seeded in fresh media and cultured for 48 h, when viability was assessed. (*D*) PDVC57 was incubated with free CPT, NNP-CPT, or BNP-CPT for 1 h. The CPT solutions were then aspirated and replaced with fresh media for 48 h, when viability was assessed. BNP-CPT increased tumor cell cytotoxicity compared to all other groups; $n = 3$. *$P < 0.05$, **$P < 0.01$, and ****$P < 0.0001$, Student's *t* test.

NPs (Fig. 3*C*). Furthermore, these results were recapitulated in a modified experiment in which PDVC57 cells were first seeded, and then incubated with either free CPT, NNP-CPT, or BNP-CPT for an hour, before the treatment volume was aspirated (*SI Appendix*, Fig. S3*B*). After a 48-h incubation, cell viability was assessed, with BNP-CPT exerting greater cellular toxicity relative to controls (Fig. 3*D*).

BNP-CPT Increases Tumor Retention and Antitumor Efficacy in a Preclinical Model. We utilized an in vivo murine model of SCC established through the intradermal transplantation of PDVC57 SCC cells into syngeneic C57BL/6 mice (23). To assess BNP retention, we first injected tumors with Cy5-conjugated NNPs or BNPs and visualized particle distribution via confocal microscopy 72 h after injection. NNPs demonstrated a punctate pattern of distribution with poor intratumoral retention proximal to injection site (Fig. 4*A*), while BNPs revealed a sustained distribution and higher retention, with an intercalating appearance within the tumor parenchyma (Fig. 4*B*). We next injected an independent set of tumors with equal doses of CPT, either as free drug suspended in intralipid (IL-CPT), or incorporated as NNP-CPT or BNP-CPT, and harvested the tumors 48 and 240 h later to assess CPT tumor retention. The vast majority of CPT injected (72%) was recovered from the BNP-CPT–treated mice 48 h after injection, but no CPT was recovered from IL-CPT–injected mice at that same time point (Fig. 4*C*). Furthermore, 240 h following injection, 45% of the CPT from the BNP-CPT–injected mice was recovered in the tumor, as compared to the undetectable levels of free CPT and NNP-CPT

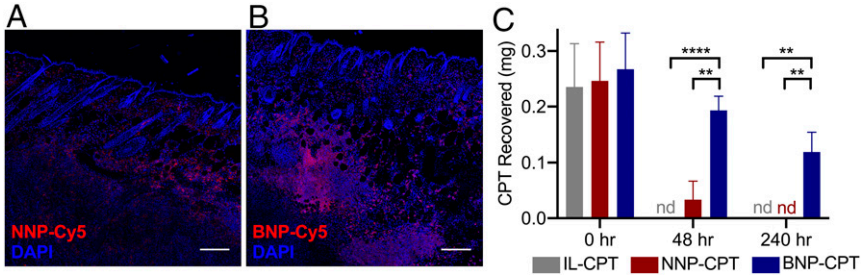

Fig. 4. BNPs exhibit greater association with tumor microenvironments in vivo to maintain local drug concentrations. Confocal microscopy of PDVC57 tumors and overlying skin 72 h after injection of NNP-Cy5 (*A*) or BNP-Cy5 (*B*). BNP-Cy5 exhibited greater intratumoral retention when compared to NNP-Cy5 (fluorescence integrated density/tissue area: NNP, 3,541.88; BNP, 10,402.26). (Scale bar: 200 μm.) (*C*) CPT recovered from tumors after treatment with intralipid-CPT (IL-CPT), NNP-CPT, or BNP-CPT. At 48 and 240 h following treatment, a greater percentage of the injected CPT was recovered from tumors treated with BNP-CPT (48 h, 72.4%; 240 h, 44.7%) when compared to free CPT (48 h, nd [not detected]; 240 h, nd) and NNP-CPT (48 h, 13.4%; 240 h, nd), indicating enhanced BNP-CPT association within SCC tumors. **$P < 0.01$, ****$P < 0.0001$, Student's *t* test; $n = 5$.

(Fig. 4*C*). Taken together, these data indicate that incorporation of CPT into BNPs markedly improves retention within tumors for up to 10 d after injection, via mechanisms that increase tumor cell binding, tumor cell uptake, and persistence within the tumor microenvironment.

To determine whether the improved intratumoral retention of BNP-CPT translated to decreased tumor burden in mice with SCCs, established tumors were treated with either blank BNPs, IL-CPT, NNP-CPT, or BNP-CPT (12.5 mg/kg CPT; Fig. 5). Animals that received BNP-CPT treatment demonstrated significantly delayed tumor growth (Fig. 5*B*) and reduced tumor weight at harvest (Fig. 5*C* and *SI Appendix*, Fig. S4) when compared to control groups, confirming the advantages of BNPs in the treatment of this murine SCC model.

We reasoned that codelivery of an adjuvant immunostimulatory agent, CpG, may enhance the capacity of BNP-CPT to eradicate tumors and extend animal survival by stimulating a local immune response to aid in tumor clearance, as has been well-characterized for CpG stimulation of TLR9 in other cutaneous malignancies, including melanoma (25, 26) and cutaneous T cell lymphoma (CTCL) (27). Through tumor induction and treatment, we found that mice receiving combination therapy of BNP-CPT plus adjuvant CpG had significantly delayed tumor growth, and full, histologically confirmed resolution in 17% of the SCC tumors (*SI Appendix*, Fig. S5). In a separate experiment, mice treated with BNP-CPT plus adjuvant CpG demonstrated significantly delayed tumor growth when compared to mice treated with vehicle, blank BNPs plus adjuvant CpG, or IL-CPT plus adjuvant CpG (Fig. 5*D* and *SI Appendix*, Fig. S6), and again a portion (20%) of tumors resolved completely, confirming the therapeutic advantages of BNP delivery. These data indicate that with further optimization, local delivery of both chemotherapeutic and immunostimulatory agents represents a practical, nonsurgical approach to the treatment of KDCs.

Discussion

An ideal nonsurgical treatment of cutaneous malignancy would provide consistent tumor elimination and low recurrence rates after a simple and efficient intervention. Toward that goal, we showed in a mouse model of nodular SCC that BNP-CPT delivery improves tumor cell binding, internalization, and toxicity; enhances intratumoral retention; and increases tumor destruction

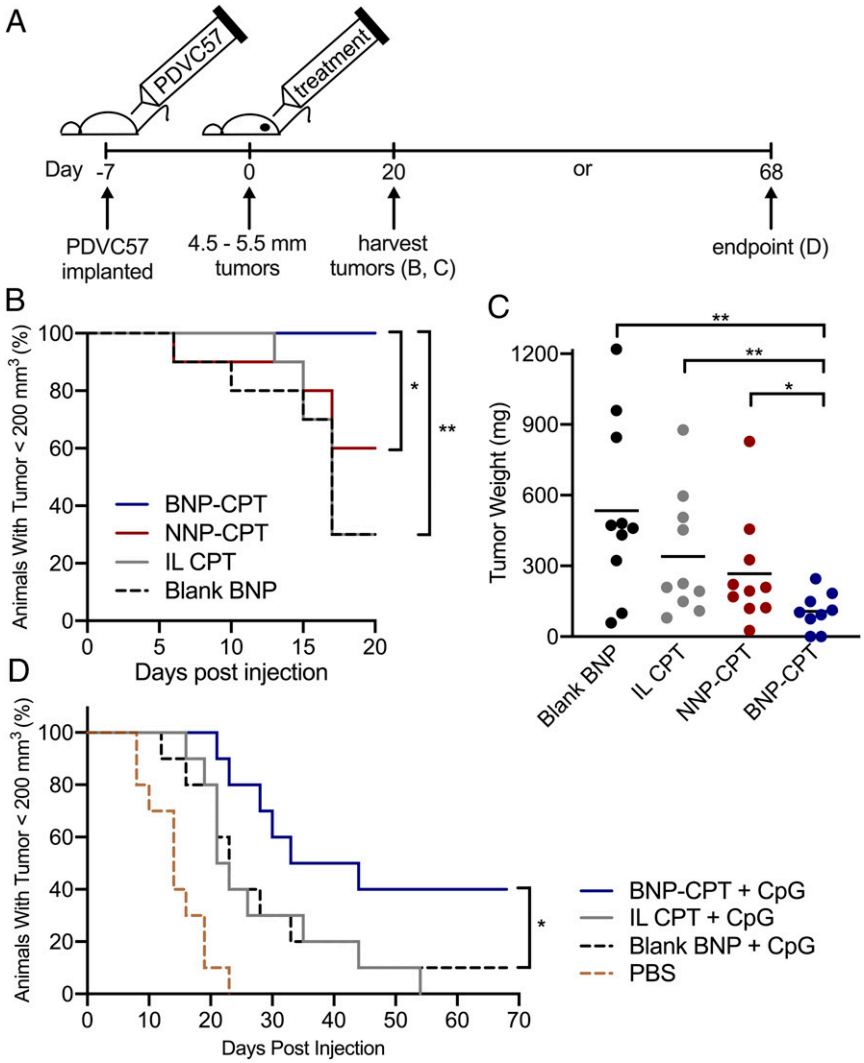

Fig. 5. Treatment of murine SCC with intratumoral BNP-CPTs is superior to NNP-CPT or intralipid-CPT. (*A*) Experiment timeline. Tumors injected with BNP-CPT showed significantly delayed tumor growth (*B*) and reduced tumor weight at harvest (*C*) (*SI Appendix*, Fig. S4) when compared to groups treated with either blank BNPs, IL-CPT, or NNP-CPT. (*D*) Combination therapy with BNP-CPT (12.5 mg/kg CPT) plus the TLR9 agonist, CpG (10 μg), significantly delayed tumor growth. $*P < 0.05$, $**P < 0.01$, Student's *t* test (*C*), Mantel–Cox test (*B* and *D*; $n = 10$).

and elimination. We further demonstrated the compatibility of BNP-CPT with coinjection of the Toll-like receptor 9 (TLR9) agonist CpG, as a combination tumor destruction plus immunotherapy; this combined approach suggests a complementary strategy that may ultimately be necessary in the clinical setting to minimize tumor recurrence risk.

Encapsulation of agents provides several advantages over free drug delivery, including to the skin (28, 29). Although nanocapsules and NPs can be synthesized from a variety of materials including ceramics, carbons, and metals (e.g., titanium, silver, gold) (30), the use of biodegradable polymers offers distinct advantages. Readily degraded in vivo through both enzymatic and nonenzymatic processes, PLA-derived lactic acid is easily eliminated by existing metabolic pathways (31). For this reason, synthetic, biodegradable polymers such as poly(lactic acid) (PLA) and poly(lactic-coglycolic acid) (PLGA) are common in biomedical applications, e.g., coating of cardiothoracic stents, bioresorbable sutures, and orthopedic, implantable fixtures, plates, and screws (32, 33). Based on prior work, we estimate that this PLA will fully degrade after a period of 6 to 12 mo (34) and that similar block copolymers of PLA and PEG have been administered to nonhuman primates and humans with no signs of toxicity (35). Similarly, HPG because of its biocompatibility is also widely utilized as an imaging reagent and for the coating of medical devices (36–38). Through both in vitro and in vivo interrogations, we confirmed that unloaded, blank PLA-HPG NNPs and BNPs did not demonstrate any observable clinical or histologic cytotoxicity.

Another vital advantage of using a synthetic polymer is the flexibility allowed in the choice of materials that form the core and the surface. Here, we have used a block copolymer of PLA and HPG, which allowed us to create NPs with a hydrophobic core and hydrophilic shell, which could be modified for avid bioadhesion. We encapsulated CPT in the hydrophobic core. Although CPT has demonstrated close to 100% growth inhibition in human malignant melanoma, breast, lung, and ovarian cancer xenografts (39, 40), there have been significant challenges with the use of CPT in the clinical setting. As a free drug, CPT is difficult to administer because of its poor solubility and rapid inactivation by hydrolysis of its lactone ring at physiologic pH (24). Encapsulation into NPs protects CPT and allows the slow release of bioactive drug. In our SCC model, encapsulation within NNPs and BNPs resulted in significantly greater antitumor effects (both in culture and in vivo) relative to CPT suspended in intralipid, suggesting the potential stabilizing and solubilizing effects of encapsulation.

The HPG shell of the NPs provides surface vicinal diols amenable to oxidative conversion to aldehydes, thereby allowing for Schiff bases to form with amines present on the cell membranes and within the protein-rich tumor matrix (19, 20). The aldehyde-rich BNPs could readily bind tumor cell surface molecules to facilitate cellular entry, where active agents may more efficiently exert direct cytotoxicity. Thus, by using BNPs sustained drug release is enhanced through tumor cell uptake as well as a depot effect within the tumor parenchyma to result in an efficient, nonsurgical, localized drug delivery to SCCs. We note a disparity in the duration of release of CPT from our NPs in vitro (Fig. 1*C*) and in vivo (Fig. 4*C*). This difference between patterns of release in vitro to in vivo is a common finding in the literature (41–43), although methods to reliably measure in vivo release are not always available. Some specialized methods have been developed (42, 44). In our studies, we were able to estimate in vivo release by using a surrogate measure of local retention in the target tissue. In the future, it will be important to distinguish between retention of free drug vs. drug within NPs, although since we know from our control experiments that free drug is cleared from the tissue within a day, we infer that the majority of drug detected at day 10 is in NPs. We measured in vitro release to assure that the BNP conversion did not alter the release properties of the NP material (Fig. 1*C*), and we use this test to confirm the quality of all of our NP formulations. We believe that the long retention of CPT after intratumoral injection in vivo represents the results of several processes, particularly internalization of BNPs into tumor cells, retention in cells, and slow release in the complex intracellular environment. It is also possible that accumulation of a protein corona on the BNPs provides another barrier slowing release.

Our in vitro data revealed the markedly enhanced tumor cell internalization of BNPs over NNPs (Figs. 2 and 3). While previous studies have suggested various endocytic mechanisms of cellular uptake by PLA-based NPs, such as clathrin-mediated endocytosis and macropinocytosis (45, 46), our results suggest that BNPs are internalized through largely clathrin-mediated endocytosis (Fig. 3). Of note, despite equal baseline fluorescence levels between dye-conjugated BNPs and NNPs, we observed that media-supplemented serum proteins (i.e., that may be required to maintain cell viability for certain assays) disparately affected internalization (*SI Appendix*, Fig. S2). Relative to serum-free media conditions, serum-containing media appeared to slow internalization of BNPs at earlier time points of coincubation and increase internalization of BNPs at later time points. In culture media prepared without added serum (Fig. 2*B*), BNP show preferential association with tumor cells. However, in serum-containing medium at early time points (Fig. 3*A*, 37 °C), this BNP preference over NNP is not observed. It is possible that BNP binding to serum proteins may delay cellular association or uptake, or that coculture in the absence of serum may activate additional uptake mechanisms. Nonetheless, at later time points (24 to 72 h; Fig. 2*C*) even in the presence of serum, BNP demonstrate a large tumor cell uptake advantage over NNP. Thus, BNP binding to serum proteins may have pleiotropic effects on tumor cell internalization in vitro; however, the relevance of this phenomenon to in vivo tumor cell uptake is unclear.

BNPs exhibited a widespread intratumoral distribution 72 h after injection and resulted in the persistent presence of encapsulated CPT 10 d after injection. A single injection of BNPs loaded with CPT produced a significant reduction in tumor burden, and complete eradication of a proportion of tumors when treated with combination BNP-CPT and CpG. Immunostimulatory agents such as CpG have demonstrated efficacy in treating a variety of cancers (47, 48). Short, single-stranded, unmethylated DNA molecules primarily found in the microbial genome, CpGs activate TLR9 in mammalian cells (49) and have demonstrated significant antitumor activity in the treatment of cutaneous malignancies such as CTCL and melanoma (25–27). Local injections of CpG into the stage I–II melanoma following surgical excision revealed improved recurrence-free survival at a median follow-up of 88.8 mo when compared to saline control (26). Furthermore, this same study reported that even in the absence of surgical excision, intratumoral injection of CpG into melanoma lesions demonstrated immune-mediated tumor regression when compared to vehicle control.

Although chemotherapeutic agents like CPT may negatively affect local immune cell populations, several studies have suggested that chemotherapy-induced immune suppression may be beneficial due to an overall reduction in regulatory T cells and tumor-associated macrophages that inhibit antitumor immune responses (50, 51). Our data suggest the feasibility and augmented benefits of multimodal therapy in a single-dose treatment strategy for the local treatment of SCCs. However, further studies are required to determine the potential for synergistic antitumoral mechanisms of BNP-CPT and CpG, and whether such depletes undesirable populations of local immune cells to facilitate direct and immune-mediated tumor cytotoxicity.

Currently, the use of existing topical agents (e.g., 5-fluorouracil or imiquimod) for the treatment of superficial SCC requires significant patient compliance with multiple applications daily over a span of weeks to months. Furthermore, such topical agents do not provide for sufficient penetration or elimination of thicker, more nodular skin tumors. A single injection therapy, as might be offered by BNP-CPT, therefore has the potential to improve the logistics, safety, and efficacy of nonsurgical treatment of skin cancers like SCC.

Materials and Methods

NP Preparation. CPT-loaded NNPs were synthesized via the modified single emulsion method (52). Briefly, 95 mg of PLA-HPG was dissolved in 2.4 mL of ethyl acetate (EtOAc) overnight. Five milligrams of CPT or 0.2 wt% fluorescent dye (DiD) was dissolved in 0.6 mL of dimethyl sulfoxide (DMSO) and was added to the polymer solution, and the combined organic phase was added dropwise to 4 mL of vortexing water. The mixture was further emulsified using a probe-sonicator for four cycles at 10-s intervals. The emulsion was immediately diluted in 10 mL of water with stirring, and EtOAc was removed via rotary evaporation at room temperature (RT). NPs were collected via centrifugation at 4,000 × *g* for 30 min at 4 °C using a 100-kDa MWCO centrifugal filter and washed twice with 15 mL of water to isolate NNPs, resulting in a 75% yield. Cy5-conjugated NNPs were prepared by the same method, using the combined solution of 90 mg of PLA-HPG dissolved in 2.4 mL of EtOAc and 10 mg of Cy5-conjugated PLA (AV032; PolySciTech) dissolved in 0.6 mL of DMSO. NNPs were resuspended in 1 mL of water. Oxidative cleavage of terminal vicinal diols was achieved with modification of a previously reported procedure (18). NNP stock was diluted threefold with water to ∼25 mg/mL. One volume of NNPs in water was incubated with 1 vol of 0.1 M $NaIO_4$(aq) and 1 vol of 10× PBS on ice for 20 min. The reaction was quenched with 1 vol of 0.2 M Na_2SO_3(aq), and the resulting BNPs were isolated using a 100-kDa MWCO centrifugal filter. BNPs were washed twice with 15 mL of water.

CPT Quantification. Drug incorporation efficiency was determined through the quantification of CPT by exploiting the intrinsic fluorescence of CPT under acidic conditions, as previously described (53). Briefly, lyophilized NP were dissolved in DMSO. Ten microliters of NP were mixed with 10 μL of 1 N HCl, 10 μL of 10% SDS, and 1 mL of PBS, in that order. A standard curve was similarly prepared with known concentrations of CPT in DMSO. To quantify CPT in NP in suspension, the same assay was performed using NP (in dH_2O) diluted in DMSO at a 1:50 dH_2O:DMSO (vol/vol) ratio, and a standard curve prepared with known concentrations of CPT in a 1:50 dH_2O:DMSO (vol/vol) vehicle. In both cases, the fluorescence of CPT was measured using a SpectraMax M5 microplate reader (Molecular Devices; excitation [Ex]/emission [Em], 370/428) and compared to CPT standards to quantify CPT concentration and drug loading efficiency. The results of a comparison of the two methods are shown in *SI Appendix*, Table S2.

Assessment of Endocytic Mechanisms of NP Uptake. PDV cells were plated at a density of 30,000 cells per well in 24-well plates in complete RPMI (CRPMI) (*SI Appendix, Supplemental Materials and Methods*) and allowed to adhere. The media was then aspirated and replaced with CRPMI containing either NNP-Cy5 or BNP-Cy5 (1 mg/mL NP) for 16-h culture (37 °C, 5% CO_2). For the final 6 h of culture, vehicle (DMSO; 0.1%), chloropromazine (CPZ) (20 μM; Sigma), an inhibitor of clathrin-dependent endocytosis, or 5-(*N*-ethyl-*N*-isopropyl)-amiloride (EIPA) (50 μM; Sigma), an inhibitor of macropinocytosis, were added to the wells. At harvest, the wells were washed five times with 1× PBS before the cells were detached with Accutase. After a brief fixation in 1% PFA, cell-associated NP fluorescence was assessed by flow cytometry using Stratedigm S1000EX (Stratedigm), and data were analyzed using FlowJo v10.4 (FlowJo). Baseline fluorescence of NNP-Cy5 and BNP-Cy5 solutions was assessed using a Promega GloMax with red filter kit (Ex, 625 nm/Em, 660 to 720 nm). Confocal microscopy is described in *SI Appendix, Supplemental Materials and Methods*.

Tumor Induction. All animal procedures were conducted in accordance with Yale Institutional Animal Care and Use Committee guidelines. Mice were housed in the Yale Animal Resource Center and afforded free access to food and water. Wild-type C57BL/6J mice were obtained from The Jackson Laboratory. To prepare the animals for tumor transplantation, the dorsal right flank was shaved using electric clippers. PDVC57 cells were harvested, as described above, washed, and resuspended in 1× PBS on ice at a concentration of 5.0×10^7 cells per mL. Mice were then anesthetized in an induction chamber with 30% isoflurane in propylene glycol and the dorsal right flank injected intradermally/subcutaneously with 5.0×10^6 cells, forming a small bleb at the site of injection.

Intratumoral NP Retention. PDVC57 tumors were induced as described above. When tumors reached a diameter of ∼5 mm, they were treated with either free CPT (0.25 mg of CPT/50 μL of intralipid), NNP-CPT (0.25 mg of CPT/50 μL of PBS), or BNP-CPT (0.25 mg of CPT/50 μL of PBS). Following injection, tumors were harvested and lyophilized at 0, 48, and 240 h. Lyophilized tumors were then homogenized with the Precellys 24 Homogenizer with soft tissue homogenizing 1.4-mm ceramic beads (Bertin) for 4 min and 35 s in 45-s pulses with 500 μL of DMSO. The first 500 μL was removed and another 500 μL added for another round of homogenization. The homogenate was centrifuged at 10,000 × *g* for 5 min to pellet residual tumor and debris, the supernatant removed, and CPT quantified using its intrinsic fluorescence as described above.

In Vivo Assessment of CPT NP Efficacy. PDVC57 tumors were induced as described above. When tumors attained a diameter of ∼5 mm, they were injected with either blank BNPs (1.99 mg/50 μL of PBS), IL-CPT (0.25 mg of CPT/50 μL), NNP-CPT (0.25 mg of CPT/50 μL of PBS), or BNP-CPT (0.25 mg of CPT/50 μL of PBS) using a 27-gauge needle, which was positioned in the center of the tumor. The entire treatment volume was administered intratumorally over 15 s. The needle was then held in this position for 10 s and withdrawn slowly in order to prevent leakage of drug from the injection site. In vivo dosing was based on both literature review and our pilot studies that revealed antitumor activity (without clinical evidence of systemic toxicity) when a single dose of 0.25 mg of CPT was delivered by intratumoral injection.

Statistics. The Mantel–Cox test was used to assess Kaplan–Meier curves (Fig. 5 *B* and *D*). All other experimental groups were compared using an unpaired one-tailed Student *t* test with significance established at $P < 0.05$. All statistical analyses were performed using GraphPad Prism 8.3 software.

Data Availability. All study data are included in the article and/or *SI Appendix*.

ACKNOWLEDGMENTS. This work was supported by awards from Stradefy Biosciences, Inc. (to M.G. and W.M.S.), and an American Skin Association Hambrick Medical Student Grant (to J.K.H.).

1. F. Xiang, R. Lucas, S. Hales, R. Neale, Incidence of nonmelanoma skin cancer in relation to ambient UV radiation in white populations, 1978–2012: Empirical relationships. *JAMA Dermatol.* **150**, 1063–1071 (2014).
2. H. W. Rogers, M. A. Weinstock, S. R. Feldman, B. M. Coldiron, Incidence estimate of nonmelanoma skin cancer (keratinocyte carcinomas) in the U.S. population, 2012. *JAMA Dermatol.* **151**, 1081–1086 (2015).
3. S. K. T. Que, F. O. Zwald, C. D. Schmults, Cutaneous squamous cell carcinoma: Incidence, risk factors, diagnosis, and staging. *J. Am. Acad. Dermatol.* **78**, 237–247 (2018).
4. J. G. Muzic *et al.*, Incidence and trends of basal cell carcinoma and cutaneous squamous cell carcinoma: A population-based study in Olmsted County, Minnesota, 2000 to 2010. *Mayo Clin. Proc.* **92**, 890–898 (2017).
5. L. M. Hollestein, E. de Vries, T. Nijsten, Trends of cutaneous squamous cell carcinoma in The Netherlands: Increased incidence rates, but stable relative survival and mortality 1989–2008. *Eur. J. Cancer* **48**, 2046–2053 (2012).
6. M. G. Kosmadaki, B. A. Gilchrest, The demographics of aging in the United States: Implications for dermatology. *Arch. Dermatol.* **138**, 1427–1428 (2002).
7. R. Chockalingam, C. Downing, S. K. Tyring, Cutaneous squamous cell carcinomas in organ transplant recipients. *J. Clin. Med.* **4**, 1229–1239 (2015).
8. K. A. Burton, K. A. Ashack, A. Khachemoune, Cutaneous squamous cell carcinoma: A review of high-risk and metastatic disease. *Am. J. Clin. Dermatol.* **17**, 491–508 (2016).
9. A. N. Kauvar *et al.*, Consensus for nonmelanoma skin cancer treatment, Part II: Squamous cell carcinoma, including a cost analysis of treatment methods. *Dermatol. Surg.* **41**, 1214–1240 (2015).
10. C. C. Huang, S. M. Boyce, Surgical margins of excision for basal cell carcinoma and squamous cell carcinoma. *Semin. Cutan. Med. Surg.* **23**, 167–173 (2004).
11. V. J. Reeder *et al.*, Trends in Mohs surgery from 1995 to 2010: An analysis of nationally representative data. *Dermatol. Surg.* **41**, 397–403 (2015).
12. G. P. Guy Jr, S. R. Machlin, D. U. Ekwueme, K. R. Yabroff, Prevalence and costs of skin cancer treatment in the U.S., 2002–2006 and 2007–2011. *Am. J. Prev. Med.* **48**, 183–187 (2015).
13. A. Salim, J. A. Leman, J. H. McColl, R. Chapman, C. A. Morton, Randomized comparison of photodynamic therapy with topical 5-fluorouracil in Bowen's disease. *Br. J. Dermatol.* **148**, 539–543 (2003).

14. C. Morton *et al.*, Comparison of topical methyl aminolevulinate photodynamic therapy with cryotherapy or fluorouracil for treatment of squamous cell carcinoma in situ: Results of a multicenter randomized trial. *Arch. Dermatol.* **142**, 729–735 (2006).
15. G. K. Patel *et al.*, Imiquimod 5% cream monotherapy for cutaneous squamous cell carcinoma in situ (Bowen's disease): A randomized, double-blind, placebo-controlled trial. *J. Am. Acad. Dermatol.* **54**, 1025–1032 (2006).
16. A. Mackenzie-Wood, S. Kossard, J. de Launey, B. Wilkinson, M. L. Owens, Imiquimod 5% cream in the treatment of Bowen's disease. *J. Am. Acad. Dermatol.* **44**, 462–470 (2001).
17. P. Kishi, C. J. Price, Life-threatening reaction with topical 5-fluorouracil. *Drug Saf. Case Rep.* **5**, 4 (2018).
18. Y. Deng *et al.*, Improved i.p. drug delivery with bioadhesive nanoparticles. *Proc. Natl. Acad. Sci. U.S.A.* **113**, 11453–11458 (2016).
19. E. Song *et al.*, Surface chemistry governs cellular tropism of nanoparticles in the brain. *Nat. Commun.* **8**, 15322 (2017).
20. Y. Deng *et al.*, A sunblock based on bioadhesive nanoparticles. *Nat. Mater.* **14**, 1278–1285 (2015).
21. M. Mohideen *et al.*, Degradable bioadhesive nanoparticles for prolonged intravaginal delivery and retention of elvitegravir. *Biomaterials* **144**, 144–154 (2017).
22. H. W. Suh *et al.*, Biodegradable bioadhesive nanoparticle incorporation of broad-spectrum organic sunscreen agents. *Bioeng. Transl. Med.* **4**, 129–140 (2018).
23. C. Caulín, C. Bauluz, A. Gandarillas, A. Cano, M. Quintanilla, Changes in keratin expression during malignant progression of transformed mouse epidermal keratinocytes. *Exp. Cell Res.* **204**, 11–21 (1993).
24. V. J. Venditto, E. E. Simanek, Cancer therapies utilizing the camptothecins: A review of the in vivo literature. *Mol. Pharm.* **7**, 307–349 (2010).
25. H. M. Najar, J. P. Dutz, Topical CpG enhances the response of murine malignant melanoma to dacarbazine. *J. Invest. Dermatol.* **128**, 2204–2210 (2008).
26. B. D. Koster *et al.*, Local adjuvant treatment with low-dose CpG-B offers durable protection against disease recurrence in clinical stage I–II melanoma: Data from two randomized phase II trials. *Clin. Cancer Res.* **23**, 5679–5686 (2017).
27. Y. H. Kim *et al.*, Phase I trial of a Toll-like receptor 9 agonist, PF-3512676 (CPG 7909), in patients with treatment-refractory, cutaneous T-cell lymphoma. *J. Am. Acad. Dermatol.* **63**, 975–983 (2010).
28. V. Krishnan, S. Mitragotri, Nanoparticles for topical drug delivery: Potential for skin cancer treatment. *Adv. Drug Deliv. Rev.* **153**, 87–108 (2020).
29. M. R. Prausnitz, Engineering microneedle patches for vaccination and drug delivery to skin. *Annu. Rev. Chem. Biomol. Eng.* **8**, 177–200 (2017).
30. J. Jeevanandam, A. Barhoum, Y. S. Chan, A. Dufresne, M. K. Danquah, Review on nanoparticles and nanostructured materials: History, sources, toxicity and regulations. *Beilstein J. Nanotechnol.* **9**, 1050–1074 (2018).
31. Y. Lu, S. C. Chen, Micro and nano-fabrication of biodegradable polymers for drug delivery. *Adv. Drug Deliv. Rev.* **56**, 1621–1633 (2004).
32. T. Casalini, F. Rossi, A. Castrovinci, G. Perale, A perspective on polylactic acid-based polymers use for nanoparticles synthesis and applications. *Front. Bioeng. Biotechnol.* **7**, 259 (2019).
33. B. Tyler, D. Gullotti, A. Mangraviti, T. Utsuki, H. Brem, Polylactic acid (PLA) controlled delivery carriers for biomedical applications. *Adv. Drug Deliv. Rev.* **107**, 163–175 (2016).
34. R. A. Miller, J. M. Brady, D. E. Cutright, Degradation rates of oral resorbable implants (polylactates and polyglycolates): Rate modification with changes in PLA/PGA copolymer ratios. *J. Biomed. Mater. Res.* **11**, 711–719 (1977).
35. J. Hrkach *et al.*, Preclinical development and clinical translation of a PSMA-targeted docetaxel nanoparticle with a differentiated pharmacological profile. *Sci. Transl. Med.* **4**, 128ra39 (2012).
36. D. Wilms, S. E. Stiriba, H. Frey, Hyperbranched polyglycerols: From the controlled synthesis of biocompatible polyether polyols to multipurpose applications. *Acc. Chem. Res.* **43**, 129–141 (2010).
37. R. K. Kainthan, S. R. Hester, E. Levin, D. V. Devine, D. E. Brooks, In vitro biological evaluation of high molecular weight hyperbranched polyglycerols. *Biomaterials* **28**, 4581–4590 (2007).
38. R. K. Kainthan, D. E. Brooks, In vivo biological evaluation of high molecular weight hyperbranched polyglycerols. *Biomaterials* **28**, 4779–4787 (2007).
39. B. C. Giovanella *et al.*, Complete growth inhibition of human cancer xenografts in nude mice by treatment with 20-(*S*)-camptothecin. *Cancer Res.* **51**, 3052–3055 (1991).
40. M. E. Wall, M. C. Wani, Camptothecin and Taxol: Discovery to clinic—Thirteenth Bruce F. Cain Memorial Award Lecture. *Cancer Res.* **55**, 753–760 (1995).
41. N. Kamaly, B. Yameen, J. Wu, O. C. Farokhzad, Degradable controlled-release polymers and polymeric nanoparticles: Mechanisms of controlling drug release. *Chem. Rev.* **116**, 2602–2663 (2016).
42. K. M. Laginha, S. Verwoert, G. J. Charrois, T. M. Allen, Determination of doxorubicin levels in whole tumor and tumor nuclei in murine breast cancer tumors. *Clin. Cancer Res.* **11**, 6944–6949 (2005).
43. J. Cui *et al.*, Ex vivo pretreatment of human vessels with siRNA nanoparticles provides protein silencing in endothelial cells. *Nat. Commun.* **8**, 191 (2017).
44. Y. Zhang *et al.*, Non-invasive, real-time reporting drug release in vitro and in vivo. *Chem. Commun. (Camb.)* **51**, 6948–6951 (2015).
45. B. Yameen *et al.*, Insight into nanoparticle cellular uptake and intracellular targeting. *J. Control. Release* **190**, 485–499 (2014).
46. L. P. Fernando *et al.*, Mechanism of cellular uptake of highly fluorescent conjugated polymer nanoparticles. *Biomacromolecules* **11**, 2675–2682 (2010).
47. H. Fan *et al.*, Intracerebral CpG immunotherapy with carbon nanotubes abrogates growth of subcutaneous melanomas in mice. *Clin. Cancer Res.* **18**, 5628–5638 (2012).
48. I. Sagiv-Barfi *et al.*, Eradication of spontaneous malignancy by local immunotherapy. *Sci. Transl. Med.* **10**, 426 (2018).
49. X. Du, A. Poltorak, Y. Wei, B. Beutler, Three novel mammalian Toll-like receptors: Gene structure, expression, and evolution. *Eur. Cytokine Netw.* **11**, 362–371 (2000).
50. M. E. Lutsiak *et al.*, Inhibition of $CD4^+25^+$ T regulatory cell function implicated in enhanced immune response by low-dose cyclophosphamide. *Blood* **105**, 2862–2868 (2005).
51. F. Ghiringhelli *et al.*, $CD4^+CD25^+$ regulatory T cells suppress tumor immunity but are sensitive to cyclophosphamide which allows immunotherapy of established tumors to be curative. *Eur. J. Immunol.* **34**, 336–344 (2004).
52. Y. Deng *et al.*, The effect of hyperbranched polyglycerol coatings on drug delivery using degradable polymer nanoparticles. *Biomaterials* **35**, 6595–6602 (2014).
53. J. Liu, Z. Jiang, S. Zhang, W. M. Saltzman, Poly(omega-pentadecalactone-co-butylene-co-succinate) nanoparticles as biodegradable carriers for camptothecin delivery. *Biomaterials* **30**, 5707–5719 (2009).